Probing the Microstructure of Nonionic Microemulsions with Ethyl Oleate by Viscosity, ROESY, DLS, SANS, and Cyclic Voltammetry

ARTICLE *in* LANGMUIR · JUNE 2012

Impact Factor: 4.46 · DOI: 10.1021/la300540d · Source: PubMed

6 AUTHORS, INCLUDING:

Leonardo Chiappisi
Institut Laue-Langevin
20 PUBLICATIONS **121** CITATIONS
SEE PROFILE

Sylvain François Prévost
European Synchrotron Radiation Facility
67 PUBLICATIONS **573** CITATIONS
SEE PROFILE

Ralf Schweins
Institut Laue-Langevin
127 PUBLICATIONS **1,652** CITATIONS
SEE PROFILE

Michael Gradzielski
Technische Universität Berlin
203 PUBLICATIONS **3,392** CITATIONS
SEE PROFILE

Langmuir

Article

pubs.acs.org/Langmuir

Probing the Microstructure of Nonionic Microemulsions with Ethyl Oleate by Viscosity, ROESY, DLS, SANS, and Cyclic Voltammetry

Gurpreet Kaur,[†] Leonardo Chiappisi,[‡] Sylvain Prévost,[‡,§] Ralf Schweins,[∥] Michael Gradzielski,*[,‡] and Surinder K. Mehta*[,†]

[†]Department of Chemistry and Centre for Advanced Studies in Chemistry, Panjab University, Chandigarh-160014, India

[‡]Stranski-Laboratorium für Physikalische und Theoretische Chemie, Institut für Chemie, Technische Universität Berlin, D-10623 Berlin, Germany

[§]Helmholtz-Zentrum Berlin (HZB), D-14109 Berlin, Germany

[∥]Institut Laue-Langevin (ILL), DS/LSS Group, F-38042 Grenoble, France

Supporting Information

ABSTRACT: Microemulsions are important formulations in cosmetics and pharmaceutics and one peculiarity lies in the so-called "phase inversion" that takes place at a given water-to-oil concentration ratio and where the average curvature of the surfactant film is zero. In that context, we investigated the structural transitions occurring in Brij 96-based microemulsions with the cosmetic oil ethyl oleate and studied the influence of the short chain alcohol butanol on their structure and properties as a function of water addition. The characterization has been carried out by means of transport properties, spectroscopy, DLS, SANS, and electrochemical methods. The results confirm that the nonionic Brij 96 in combination with butanol as cosurfactant forms a U-type microemulsion that upon addition of water undergoes a continuous transition from swollen reverse micelles to oil-in-water (O/W) microemulsion via a bicontinuous region. After determining the structural transition through viscosity and surface tension, the 2D-ROESY studies give an insight into the microstructure, i.e., the oil component ethyl oleate mainly is located at the hydrophobic tails of surfactant while butanol molecules reside preferentially in the interface. SANS experiments show a continuous increase of the size of the structural units with increasing water content. The DLS results are more complex and show the presence of two relaxation modes in these microemulsions for low water content and a single diffusive mode only for the O/W microemulsion droplets. The fast relaxation reflects the size of the structural units while the slower one is attributed to the formation of a network of percolated microemulsion aggregates. Electrochemical studies using ferrocene have been carried out and successfully elucidated the structural transformations with the help of diffusion coefficients. An unusual behavior of ferrocene has been observed in the present microheterogeneous medium, giving a deeper insight into ferrocene electrochemistry. NMR-ROESY experiments give information regarding the internal organization of the microemulsion droplets. In general, one finds a continuous structural transition from a W/O over a bicontinuous to an O/W microemulsion, however with a peculiar network formation over an extended concentration range, which is attributed to the somewhat amphiphilic oil ethyl oleate. The detailed knowledge of the structural behavior of this type of system might be important for their future applications.

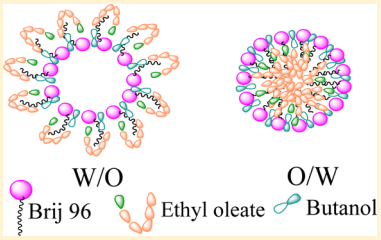

INTRODUCTION

Different colloidal assemblies such as micellar systems, microemulsions, vesicles, etc. have been extensively studied as carrier systems for active agents because of their unique properties that combine hydrophilic and hydrophobic domains within one homogeneous solution. Correspondingly, there has been widespread interest in studying the physicochemical properties of different self-assembled systems with the perspective to use them in a large variety of applications and formulations.[1] In particular, this is the case for microemulsions, which are thermodynamically stable mixtures of oil and water facilitated by the presence of surfactant, and where an enormous amount of work has been done since they were first described by Schulman et al.[2] in 1943. As an example, recently biocompatible microemulsions for encapsulation and delivery have been reviewed.[3]

One of the unique factors associated with microemulsions is the variability of their structural types such as oil droplets in water (O/W), water droplets in oil (W/O), or bicontinuous structures, which are formed depending on the curvature of the interface, which is controlled by different factors such as salinity, temperature, etc.[4−6] Accordingly, the structure of microemulsions is a function of these parameters as well as of the composition of the system. In principle, the formation of microemulsions is connected to having a low interfacial tension,[4,6,7] and therefore, their free energy is governed by the bending energy of their surfactant monolayer,[8−11] which then allows for a rational and self-consistent interpretation of

Received: February 6, 2012
Revised: June 18, 2012
Published: June 21, 2012

the structural features of microemulsions based on the bending constants of the monolayer.[11−13]

One peculiarity of microemulsions lies in the fact that its continuous phase is interchangeable, i.e., W/O vs O/W can be formed within one surfactant/oil/water system,[14] but their application demands the identification of the respective structures and of the structural transitions occurring in these systems with dilution and/or in presence of an additive, which might be needed for a certain application or is admixed in order to achieve required structural properties. The classification of microemulsions into S-type and U-type as coined by Clausse holds a significant importance from the view of their capability to solubilize a drug or food component. The S-type microemulsion system contains domains in disjoined regions in the phase diagram, whereas in the U-type system the dilution with aqueous phase progressively inverts the structure from the oil rich side to water rich via a bicontinuous structure without phase separation.[15] Therefore, precise knowledge of their microstructure is of great importance, and many attempts have been made concerning the relationship between microemulsion structure and measurable physical properties.[13−17] For a complete understanding of the microstructure, typically the combination of a variety of complementary techniques is required, and correspondingly, a large arsenal of different methods has been employed.[1,17−19] Among the many applications of microemulsions, one important area is the field of drug delivery. Recent literature witnesses many successful examples of pharmaceutically acceptable microemulsions as drug carriers.[20] However, for their use in drug delivery, dilutability by water is a major point. The present work deals with the formation of fully dilutable Brij 96 microemulsions containing a pharmaceutically acceptable hydrophobic phase. Various alcohols (n = 2−6) have been used to tune the properties of the interface to achieve the dilutability. Cosurfactants have been shown before to be very effective in controlling the properties of microemulsions, as they allow for modifying the bending elastic properties of microemulsions, where this effect depends largely on the chain length of the cosurfactant and on its concentration.[21] Accordingly, microemulsions for pharmaceutical purposes have been formulated with isopropyl myristate and nonionic surfactants (Tween 20, 40, and 80 and Span 20) with the help of isobutanol as cosurfactant. In this system a rather large L_2-phase is formed, which then for higher water content converts into an O/W emulsion.[22]

In the present investigation, as components for the formulation of a pharmaceutically acceptable system,[23−26] we have employed ethyl oleate (EO) as oil, Brij 96 as nonionic surfactant, and ethanol to hexanol as cosolvents or cosurfactants, where however after some general scans we concentrated on butanol as cosurfactant. Such longer-chain esters are challenging for the formulation of microemulsions, as it is well-known that for instance triglycerides are very difficult to be formulated in the form of microemulsions[27] and the simple medium- and long-chain esters have more or less pronounced amphiphilic character.[28] The characterization of these systems has been done by the combination of complementary methods like viscosity, surface tension, dynamic light scattering (DLS), small-angle neutron scattering (SANS), ^{1}H NMR rotating frame nuclear Overhauser effect spectroscopy (ROESY), and cyclic voltammetry. Our basic interest lies in finding how the added water affects the microstructure of these microemulsions, thereby having the ability to control this microstructure by the extent of water addition to a given mixture of surfactant/cosurfactant/oil.

EXPERIMENTAL SECTION

Materials. Brij 96 (polyoxyethylene-10-oleoyl ether), ethanol, and hexanol were purchased from Fluka. Purity and composition of Brij 96 were elucidated with ^{1}H NMR, ^{13}C NMR, and MS. Details have been given in the Supporting Information (Figure S1). Propanol (purity >99.8%), butanol (purity >99.8%), and pentanol (purity >98%), were purchased from Spectrochem. Ethyl oleate (EO), D_2O (for NMR), NaCl, and $Fe(C_5H_5)_2$ were obtained from Sigma, while the D_2O (99.9% isotopic purity) for the SANS experiments was from Eurisotop. All chemicals were used as received. Doubly distilled water (specific conductance, 2−4 μS cm^{-1} at 303 K) was used for all preparations.

Methods. *Microemulsion Preparation and Phase Behavior.* Microemulsions consisting of oil ethyl oleate (EO), surfactant (Brij 96), alcohol, and double distilled water were prepared with a constant surfactant:cosurfactant mass ratio (K_m) of 1.5. Samples preparation was carried out in screw-cap glass vials and the temperature was maintained at 303.15 ± 0.01 K using a RE320 Ecoline thermostat. First, the oil was admixed to the surfactant:cosurfactant mixture, yielding a homogeneous solution, followed by the addition of the required amount of water to obtain the desired microemulsion compositions. The compositions were monitored visually every day for a month. Transparent, single-phase mixtures stable for over 6 months were designated as microemulsions (1Φ). The multiphase region included two-phase, three-phase, opalescent, and turbid states. The mapped phase diagram of the systems shown as Figure 1 is from our previous work.[29]

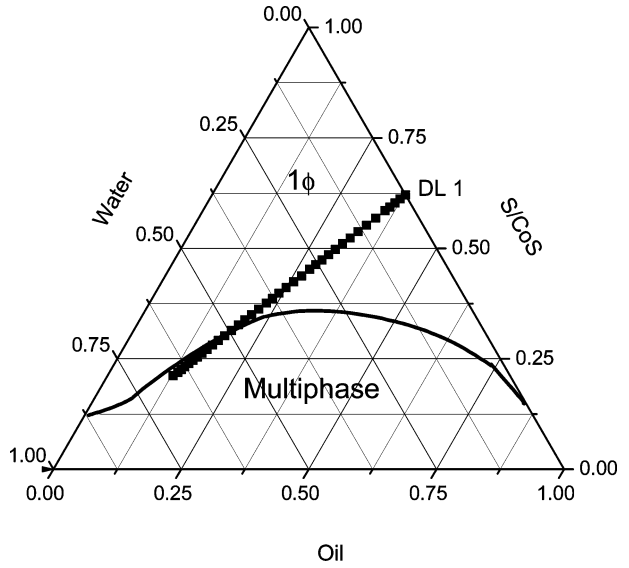

Figure 1. Phase diagram of Brij 96/butanol/water with ethyl oleate at K_m = 1.5, showing the dilution line DL 1 (as dotted points).

The elucidation of the microstructure has been carried out along a dilution line of constant oil:surfactant mixing ratio of 1.2:2 by weight. The phase behavior of the butanol system was also mapped.[29]

Optical Transparency. The homogeneity and optical isotropy of microemulsions were examined by crossed polarizers and visual examinations after the samples were thermostated in a water bath at 25 °C for 24 h, in order to achieve equilibrium conditions.

Centrifugation. Stability of microemulsions was tested by carrying out centrifugation (Tarson) at 2000 rpm for 30 min.

Viscosity. Viscosity measurements were made using a modified form of an Ubbelohde viscometer placed in a water thermostat, the temperature of which was controlled to 25 ± 0.1 °C. The viscometer was calibrated prior to the measurements by using the n-alkanols, i.e., hexanol, heptanol, and nonanol. The viscosity η was calculated using

dx.doi.org/10.1021/la300540d | Langmuir 2012, 28, 10640−10652

$$\eta = A\rho t - \frac{B\rho}{t} \quad (1)$$

where A and B are viscometer constants and were calculated as

$$A = \frac{r^4 hg}{8V(L + nr)} = \text{constan t} \quad (2)$$

$$B = \frac{mV}{8\pi(L + nr)} = \text{constan t} \quad (3)$$

where r is the radius of the capillary in cm, V the volume of the liquid in cm^3 which flows through the capillary, t is time of flow in seconds, and L is the length of the capillary in cm. ρ is density of the liquid, n is a coefficient associated with flow at the end of the capillary, and m is another coefficient associated with flow at the end of the capillary.

The determined values of the coefficients A and B are 0.0427 and −39.878, respectively. The flow time of a specified volume of liquid through the capillary was measured with a stopwatch with a resolution of 0.01 s. The measurements were repeated in triplicate to get the concordant readings. The measurement of viscosity has a precision of ±0.05% and uncertainty of ±0.2%.

Surface Tension. A Krüss Easy dyne tensiometer (K 20) was employed to determine the surface tension with the de Nuoy ring method. The ring was heated in a flame until it was red hot prior to every measurement. The experimental error is ±0.1 mN m^{-1}.

Density. Densities were measured by making use of a precision densimeter Anton Paar (model DSA 5000) at 30 ± 0.001 °C. The densimeter was calibrated before and after each set of density measurements using the density of air and water. Precision in the density has been estimated to be 1×10^{-6} g L^{-1}.

Dynamic Light Scattering. DLS experiments were performed using an ALV/CGS-3 compact goniometer system with a He−Ne laser (λ = 632.8 nm) equipped with two Avalanche photodiodes (APD) for pseudo-cross-correlation to obtain the intensity autocorrelation function $g^{(2)}(\tau)$. All measurements were performed at scattering angles between 45° and 150°, resulting in different magnitudes of the scattering vector q

$$q = \frac{4\pi n \sin(\theta/2)}{\lambda} \quad (4)$$

with n being the refractive index of the solvent, θ the scattering angle, and λ the wavelength of the light. The sample cell was kept in a toluene bath at a constant temperature of 25 °C.

The data were analyzed with a biexponential function to describe the intensity autocorrelation function $g^{(2)}(\tau)$ as

$$g^{(2)}(\tau) = A[B\exp(-2\Gamma_1\tau) + (1 - B)\exp(-2\Gamma_2\tau)] \quad (5)$$

where Γ_1 and Γ_2 are the characteristic relaxation rates of the two relaxation processes and B is their weighting factor (A being the total amplitude).

In addition, a second-order cumulant analysis on the fast decay was also performed, where the intensity autocorrelation function is described as

$$\ln(g^{(2)}(\tau)) = A - 2\Gamma_1\tau + \mu\tau^2 \quad (6)$$

The polydispersity index p is given by

$$p = \frac{\sqrt{\langle\Gamma_1^2\rangle - \langle\Gamma_1\rangle^2}}{\langle\Gamma_1\rangle} = \sqrt{\frac{\mu}{\Gamma_1^2}} \quad (7)$$

The relaxation rates can be related to the corresponding diffusion coefficients via

$$D_i = \frac{\Gamma_i}{q^2} \quad (8)$$

The diffusion coefficient D then again can be related to an effective hydrodynamic radius $R_{h,i}$ according to the Stokes−Einstein equation

$$R_{h,i} = \frac{kT}{6\pi\eta D_i} \quad (9)$$

where k is the Boltzmann constant, T the temperature, η the viscosity of the solvent, and D_i the respective diffusion coefficient.

Small-Angle Neutron Scattering. SANS experiments were done on instrument D11 of the Institut Laue-Langevin (ILL), Grenoble, France. Neutrons were recorded on a two-dimensional ^{3}He gas detector of 128 × 128 pixels of 7.5 × 7.5 mm^2. The wavelength was 6 Å (fwhm 10%), a collimation length of 8 m was chosen, and sample-to-detector distances of 1.2 and 8 m were selected, thereby covering a range of the magnitude of the wave vector q = 0.006−0.5 $Å^{-1}$. Samples were contained in quartz cuvettes of QS quality (Hellma) of 1 mm path length, placed in a thermostated (25.0 ± 0.1 °C) sample changer.

Raw data were corrected for the scattering of the empty cell. The detector efficiency and solid angle variations were taken into account by dividing with the scattering pattern of a 1 mm water sample. All raw data were corrected for the scattering of the empty cell, background noise (from measurements with boron carbide (B4C) at the sample position), and corrected with the corresponding transmissions. The absolute scale was achieved by comparing with the scattering of a 1 mm water sample, assuming that all nontransmitted neutrons are scattered uniformly over the full solid angle and considering the Jacrot factor that accounts for the wavelength-dependent forward scattering of water,[30] which is $d\Sigma/d\Omega$ = 0.983 cm^{-1} under the used experimental conditions. The reduced data obtained by using the BerSANS program[31] were always isotropic and consequently azimuthally averaged. Spectra from different configurations for each sample were merged with no need of any scaling factor. The presented SANS curves still contain the incoherent background scattering of the solvent and the sample.

Cyclic Voltammetry. Cyclic voltammetric measurements were performed using an electrochemical analyzer (Autolab). A gold working electrode, a Ag/AgCl reference electrode, and a platinum counter electrode were used to carry out electrochemical measurements. The gold working electrode was polished using 0.05 mm size aluminum oxide slurries and then washed carefully with distilled water. The microemulsion system was assessed using ferrocene as probe ($Fe(C_5H_5)_2$) and NaCl as supporting electrolyte; the electrode area (A) was 3.14×10^{-6} m^2. The potential was scanned between 0 and 0.8 V, and the sweep rate range used was 20−100 mV s^{-1} in this work. The experiments were carried out under a nitrogen atmosphere to avoid the effect of oxygen. The titration method was adopted to perform the experiment at 25 °C. Initially Brij 96 (4.8 g), ethyl oleate (4.8 g), and butanol (3.2 g) were mixed with dissolved ferrocene (2.0 mM), and dilution was carried out with 0.01 M NaCl solution.

For the determination of the diffusion coefficient D of the electroactive probe by cyclic voltammetry, the peak current for a reversible system is described by the Randles−Sevčik equation[32]

$$I_p = 0.4463zFAc_0(nF/RT)^{1/2}D^{1/2}v^{1/2} \quad (10)$$

where z is the number of electrons involved in oxidation or reduction, F the Faraday constant, A the area of the electrode, c_0 the concentration of electroactive probe, R the gas constant, T the temperature, v the scan rate (V s^{-1}), and I_p the peak current. It follows from eq 10 that I_p will increase linearly with the square root of the scan rate. For a given electrode area and a constant probe concentration, a plot of I_p versus $v^{1/2}$ should give a straight line and D can be calculated from the slope of this line.

NMR. NMR spectra were recorded on a Bruker Avance II 400 spectrometer operating at 400 MHz. Chemical shifts were determined using D_2O as internal locking agent for ^{1}H and ROESY NMR. Tetramethylsilane (TMS) was used as an external chemical shift reference. The 2D-ROESY spectra were measured with the standard Bruker software acquisition program roesytp in the phase-sensitive mode. The spectrometer was fitted with a 5 mm PABBO BB probe head with z-gradients. The standard two-dimensional ROESY pulse sequence was used with a low-power spin-lock pulse. A relaxation delay of 2 s was used between the scans. The spin-lock field strength

dx.doi.org/10.1021/la300540d | Langmuir 2012, 28, 10640−10652

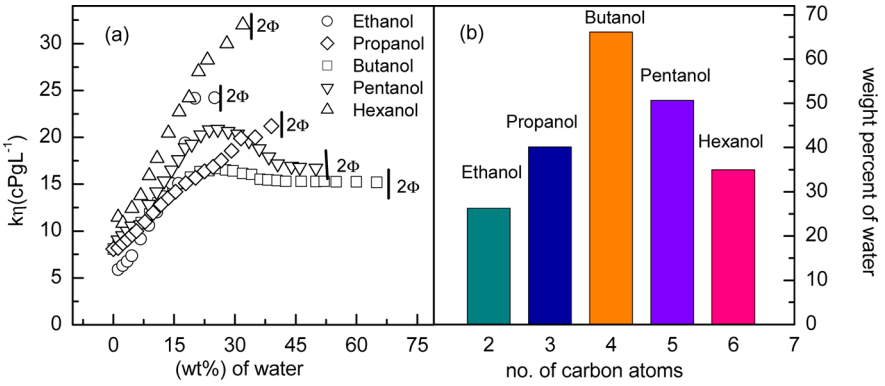

Figure 2. Variation of the (a) kinematic viscosity as a function of the weight percent (wt %) of added water and (b) water solubilization for Brij 96/ethyl oleate with different alcohols (Brij 96:butanol weight ratio of 1.5) at constant oil:surfactant mixing ratio of 1.2:2 by weight.

was 2857 Hz with a mixing time of 200 ms. Phase-sensitive two-dimensional time domains were recorded and were processed using TPPI protocol. A sine apodization function (ssb = 2) was applied in both dimensions before Fourier transformation.

RESULTS AND DISCUSSION

Visual Appearance—Phase Behavior. Initially a visual inspection of microemulsion formulated with Brij 96, ethyl oleate, and butanol (with a constant 3:1 surfactant to cosurfactant weight ratio) with varying weight percent of water was made in order to obtain a macroscopic phase diagram which is depicted in Figure 1.

Figure S2 (Supporting Information) depicts images demonstrating the optical transparency of microemulsions at different weight fraction of water. At low weight fraction of water the samples were yellowish in color, and as the dilution progresses, the samples become increasingly colorless. At 48.4 wt % water content milkiness appears; however, the sample remains still single phase. At the emulsification failure point, i.e., at 60 wt % of water, cloudiness appears and with time the system becomes biphasic (2Φ).

Viscosity. After the visual inspection, the changes upon water dilution were investigated further using viscosity, which provides information on the macroscopic behavior of the microemulsions and is a useful tool to elucidate structural changes. The viscosity measurements were carried out using ethyl oleate as oil and alcohols of different chain length as cosurfactants.

Figure 2 depicts the viscosity as a function of the weight fraction of water (wt % water) for ethyl oleate and different alcohols. The viscosity increases with dilution in all the systems except in the case of butanol and pentanol, where it reaches a maxima and then decreases upon further dilution. In the case of the other alcohols, viz., ethanol, propanol, and hexanol, there is an early breakdown of microemulsion, i.e., phase separation occurs and the sample turns milky and therefore the viscosity cannot be measured beyond 20, 32, and 25 wt % water, respectively (Figure 2). It is interesting to note that the most pronounced increase in viscosity takes place for hexanol, followed by ethanol and then pentanol, which indicates that longer chain alcohols lead to a higher viscosity, presumably by stabilizing more anisometric aggregates, as is similarly observed for micellar aggregates.[33,34] The effect of the ethanol is less clear but might be related to a change of the activity of water, a corresponding lower extent of hydration, and thereby a tendency for more anisometric aggregates. Apparently these medium chain alcohols, which have a pronounced cosurfactant character, are most effective in producing interconnected structures with a correspondingly higher viscosity.

The maximum dilutability is achieved in the case of butanol. The ability of the cosurfactants (longer chain alcohols) to penetrate into the amphiphilic film shall be related to their efficiency in microemulsion stabilization. However, the penetration decreases as the cosurfactant becomes more hydrophobic, as is the case of hexanol. For ethanol and propanol, these shorter carbon chain alcohols are fully soluble in the aqueous phase and are therefore less to be considered as cosurfactants than as cosolvents. Since the solubility of *n*-butanol is intermediate in water, it is expected to partition preferentially toward the interfacial layer. As reported by Leung and Shah,[5] the maximum solubilization is interpreted as a result of counteracting effects of attractive interdroplet interaction of fluid interfaces and the bending stress of rigid interfaces. It is believed that the variation of water solubility with the number of carbons in the alcohol chain (nc) in the preconcentrate of the microemulsion is dependent on these factors, and butanol shows maximum solubilization. Figure 2b depicts the maximum water solubilization for the different alcohols in Brij 96/ethyl oleate microemulsion.

In general, the increase in the volume fraction of the dispersed phase in microemulsions brings about an increase in viscosity.[1,35] It is expected that the change in viscosity reflects structural transformations of the system's microstructure upon the addition of water and this has been analyzed in more detail using butanol (Figure 3). The viscosity curve along the dilution lines can be divided into three regions based on the slope (as a function of dilution). The viscosity increases initially with the amount of added water due to the formation of dispersed aggregates. At around 20 wt % water such a maximum is reached and further water addition then leads to a decreasing viscosity. After passing through a minimum (~40 wt % water), the viscosity increases again. The initial increase of viscosity with dilution is probably the consequence of attractive interactions and aggregation of droplets of water phase including molecular reorganization on the interface[35] and may indicate a change in the shape of the microemulsion aggregates.

The two transition points in the plot of $1/\eta[d\eta/d(\text{wt \% water})]$ vs wt % water (Figure S3, Supporting Information) at 6.5 and 40 wt % water can be associated with the transition of swollen reverse micelles to short cylinders and then to O/W from bicontinuous, respectively. Several structural models, such as the Voronoi polyhedron, layered structure, extended

dx.doi.org/10.1021/la300540d | *Langmuir* 2012, 28, 10640−10652

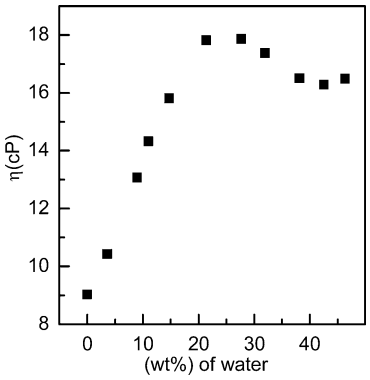

Figure 3. Variation of dynamic viscosity with weight percent of water (wt % water), for Brij 96/ethyl oleate/butanol with a Brij 96:butanol weight ratio of 1.5 and at constant oil:surfactant mixing ratio of 1.2:2 by weight.

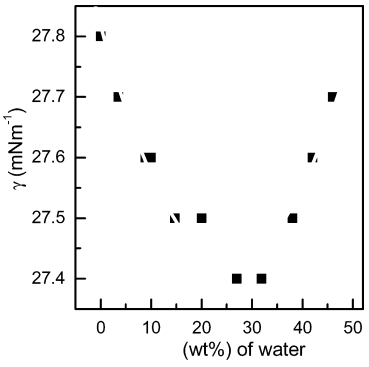

Figure 4. Variation of surface tension σ (■) with weight percent of water (wt % water) for the system Brij 96/butanol/ethlyoleate/water (for constant Brij 96:butanol weight ratio of 1.5) at constant oil:surfactant mixing ratio of 1.2:2 by weight.

structure fluctuation, and disordered open connected models, have been proposed in attempts to describe bicontinuous microemulsions.[36−38] These models, which propose that surfactants form extended films to separate water from oil, cannot interpret unambiguously why there is usually a decrease in the viscosity when the more structured bicontinuous microemulsion forms from discrete W/O or O/W microemulsion. However, it has frequently been observed experimentally that around such a transition point from a droplet to a bicontinuous microemulsion a viscosity maximum occurs.[39−41] We assume that the decrease of the viscosity values in the bicontinuous region has to be attributed to the fact that this is a highly dynamic structure, where the dynamics is enhanced due to the large amount of butanol present in the amphiphilic monolayer. The small increase in the dynamic viscosity for water contents above 48 wt % suggests a further structural transformation from a bicontinuous structure to an O/W structure. This phenomenon can be attributed to a percolated droplet structure that has to be present as the transition occurs.[36−38]

Thus, the viscosity results show the continuous transition from swollen reverse micelles (∼6 wt % water) into short cylinders and thereafter into continuous channels [between 20 and 40 wt % water (Figure S3, Supporting Information)] with the system finally reverting in O/W type (>40 wt % water) on dilution until the emulsification failure point is reached (∼60 wt % water).

Surface Tension. Measurements of surface tension and density have been carried out for the Brij 96/ethyl oleate/butanol system, and this macroscopic data is depicted in Figure 4. The density increases monotonically with increasing weight fraction of water. However, the surface tension measurements obey a polynomial fit (second order), with increasing content of the aqueous phase. The surface tension initially decreases up to 30 wt % water and then increases again. This can be seen more quantitatively from the plot of $d\gamma/d$(wt % water) as a function of the weight fraction of water (Figure S3, Supporting Information), where values around zero in the range of 10−30 wt % indicate the presence of a bicontinuous structure. It should be noted that this might be seen in analogy with the minimum observed as a function of temperature in interfacial tension of nonionic surfactants, which occurs at the phase inversion temperature (PIT),[6,7,42] where also a bicontinuous microemulsion is present, and which is typically characterized by a maximum of the solubilization capacity. The relative change here is, of course, much smaller than for corresponding interfacial tension values, but the absolute change of the tension with a reduction by 0.4 mN/m is similar.

Cyclic Voltammetry. Further confirmation of the bicontinuous structure has been obtained by the electrochemical method of cyclic voltammetric (CV) measurements which was utilized to identify structure and structural transition in our microemulsions via the self-diffusion coefficient. Ferrocene, which is completely oil soluble, was selected as electroactive probe. Since microemulsions provide a multifunctional environment for solubilization and partitioning of solute, the resulting interactions also alter the diffusional and electrochemical character of the compound. Therefore, the electrochemistry of ferrocene depends on the concentration and nature of the microheterogeneous medium. It has been observed that partitioning of electroactive probes can affect reaction potential $E_{1/2}$ directly; however, partitioning constants of probe alter local concentrations, and circuitously, changes in the microenvironment amend diffusion coefficients. Since the measured diffusion coefficients is a weighted average of the diffusion coefficients in all phases of the microemulsion, i.e., oil, water, surfactant, and cosurfactant, they reflect the molecular steps involved with charge transfer to electroactive materials in the nonpolar phases. These include diffusion of the electroactive material to the surface of the droplet, diffusion out of the surface, charge transfer to the species in the interface, and movement of the ion out of the interface into the polar phase. Therefore, diffusion coefficient is believed to be dependent on the microemulsion composition.

In present case, the diffusion coefficient of ferrocene was determined by applying eq 10 to the experimental data. A representative plot of the anodic peak current I_{pc} versus $\upsilon^{1/2}$ is given in Figure 5, and from the slope the apparent diffusion coefficient D_{app} of ferrocene was calculated at different weight percent of water and is given in Figure 6 for the Brij 96/ethyl oleate/butanol microemulsion. In this electrochemical study using ferrocene, the D_{app} increases as the weight fraction of water increases.

D_{app} of ferrocene clearly depicts the changes in the microstructure of microemulsion. The transition from W/O to O/W via bicontinuous was estimated to occur at 20 and ∼40 wt % from viscosity and other methods, respectively. In this electrochemical study using ferrocene, the D_{app} increases as the weight fraction of water increases. However, reverse behavior has been reported in the case of SDS.[43] It was expected that the

dx.doi.org/10.1021/la300540d | Langmuir 2012, 28, 10640−10652

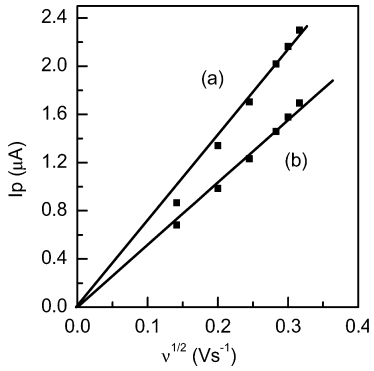

Figure 5. Representative plot of peak current I_p versus $\upsilon^{1/2}$ of Brij 96/butanol/ethyl oleate microemulsion systems (Brij 96:butanol weight ratio of 1.5), for weight percent of water of (a) 38.89% and (b) 47.9% at constant oil:surfactant mixing ratio of 1.2:2 by weight.

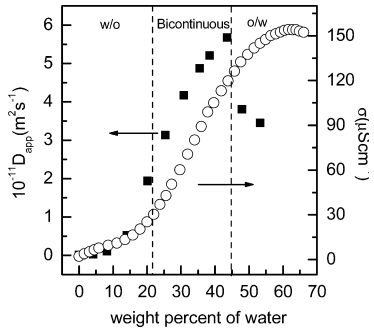

Figure 6. Diffusion coefficients of ferrocene (■) and variation of conductivity (○) for Brij 96/butanol/ethyl oleate microemulsions as a function of the water content at 25 °C.

ferrocene being oil soluble should give higher diffusion coefficients in an oil continuous medium. However, it is the partitioning behavior of ferrocene in different components of microemulsion that is responsible for the reverse trend. It is the presence of butanol in substantial amount that gives the probe a difference in solubility between different regions of a microheterogeneous system, where D in eq 10 is an apparent diffusion coefficient D_{app} that reflects the location of the ferrocene in the microheterogenous medium.

As observed from Figure 6, the value of the diffusion coefficient increases slowly in the W/O region, but beyond 18 wt % water a steep increase of D_{app} is observed. Further on then a sharp decrease is found in case of the water continuous region, i.e., above 45 wt % water. Lindman et al.[44] showed by NMR measurements that molecules in the continuous medium will be characterized by rapid diffusion. Thus, a continuous structure is expected to give a higher self-diffusion coefficient than a droplet structure. Therefore, the result of cyclic voltammetry confirms the existence of the presence of a bicontinuous structure. The shape of the curves for D and σ shows some similarities, and in particular, the transition points related to the microstructure coincide well, which confirms the presence of three distinct microstructures as a function of water content (Figure 6). The main aim in the present study is to analyze the microstructure changes occurring in microemulsion system using ferrocene as probe. It is believed that electrochemical oxidation of ferrocene (Fc) is a one-electron process forming ferricinium ion (Fc^+):

$$Fe(C_5H_5)_2 \Leftrightarrow Fe(C_5H_5)_2^+ + e^- \quad (11)$$

where one form of the probe is oil soluble (Fc) and the other (Fc^+) is water-soluble. But in this microheterogeneous environment, the electrochemical reversibility of the probe was affected by the microemulsion structure and appeared to reflect the ease of mobility across interphases. Figure S5 (Supporting Information) shows cyclic voltammograms at different scan rates with varying weight percent of water. It is observed for oil-continuous samples with less than 20 wt % water that reversibility is absent and only the reduction peak occurs. However, in the bicontinuous phase reversibility is attained with the presence of two cathodic peaks. As the dilution progresses there are two peaks in a cycle, which eventually diminishes as the system reverts to O/W.

The reason for such behavior could be the generation of ferrocenonium ion (which occurs in the presence of protic solvents). Such unusual behavior of ferrocene has been reported before by Jha et al.,[45] where contrary to the generally expected reversible peak, the experiments show the presence of a second oxidation peak during the reverse scan at low scan rates. In the present system it could be the reduction of this ferrocenonium ion initially. It is more difficult to oxidize ferrocene (easier to reduce); therefore, reversibility could not be attained.

Neutral ferrocene, which resides in the hydrophobic region, may also get trapped in the surfactant tails; therefore, as an example of Le Chatelier's principle the concentration of free ferrocene decreases in solution and thereby decreasing the diffusion coefficient. With the appearance of continuous channels (a network of water tubes in an oil matrix or a network of oil tubes in a water matrix, respectively), along with reduction of ferrocenonium ion, reversibility of ferrocene to ferricinium ion is clearly observed.

Small-Angle Neutron Scattering. In order to gain further structural insight on the mesoscopic level, SANS experiments have been done along the dilution line given in Figure 1, and the SANS spectra are given in Figure 7. One observes a continuous and substantial increase of scattering intensity with increasing water content and at the same time a correlation peak becomes increasingly prominent that shifts to lower q. This demonstrates that the structural units present become

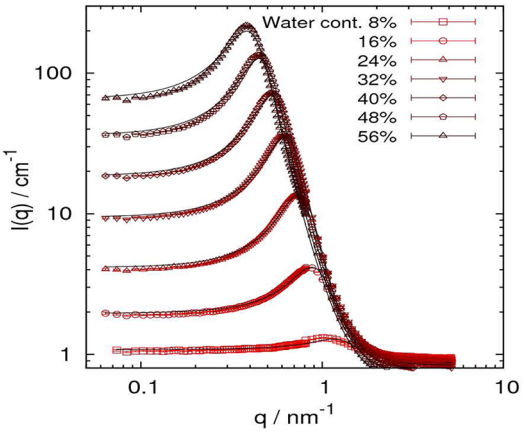

Figure 7. SANS spectra for microemulsions of the system Brij 96/ethyl oleate, with constant ratio between Brij 96/ethyl oleate and butanol of 1.5:1.5:1 as a function of the amount of added water. Full lines are fits according to the Teubner–Strey model (eqs 12 and 13).

dx.doi.org/10.1021/la300540d | Langmuir 2012, 28, 10640–10652

bigger with increasing water dilution and develop a higher degree of ordering, which is not surprising, given the relatively high volume fractions of dispersed phase.

The scattering data were modeled with the empirical Teubner–Strey model that has been employed successfully before for the description of bicontinuous microemulsions[46−49] (although it should be noted that it will also describe droplet microemulsions decently well). It allows deducing typical structural parameters as the correlation length (ξ) and the repeat distance (d) without resorting to a specific structural model. For this model the scattering intensity is given as

$$I(q) = \frac{8\pi c_2 \langle \eta^2 \rangle / \xi}{a_2 + c_1 q^2 + c_2 q^4} \tag{12}$$

$$d = 2\pi \left[\frac{1}{2}\sqrt{\frac{a_2}{c_2}} - \frac{1}{4}\frac{c_1}{c_2} \right]^{-1/2} \tag{13a}$$

$$\xi = \left[\frac{1}{2}\sqrt{\frac{a_2}{c_2}} + \frac{c_1}{4c_2} \right]^{-1/2} \tag{13b}$$

$$\langle \eta^2 \rangle = \Phi_1 \Phi_2 (\Delta\rho)^2 \tag{13c}$$

where Φ_1 and Φ_2 are the volume fractions of the two domains (hydrophilic and hydrophobic, respectively), and $\Delta\rho$ is the scattering length density difference between them.

The Teubner–Strey model allows for a very good modeling of the scattering curves (see Figure 7), and in Figure 8 and Table 1 the variation of the parameters ξ and d as a function of the water weight fraction is reported. The correlation length ξ, that is characteristic for the domain size of the scattering units, increases from ca. 2 nm to reach a plateau of ca. 8 nm for 50 wt % water, a size typically observed for microemulsions,[1] where for this high water content one may assume the presence of microemulsion droplets. The repeat distance d is linearly increasing with the amount of water contained, which means that the structures present follow a simple swelling law upon addition of water. As the leading term in the free energy of a microemulsion can be assumed to be the bending energy,[9−11,13] from ξ and d one can determine the renormalized bending rigidity κ of the oil-swollen membranes via[50]

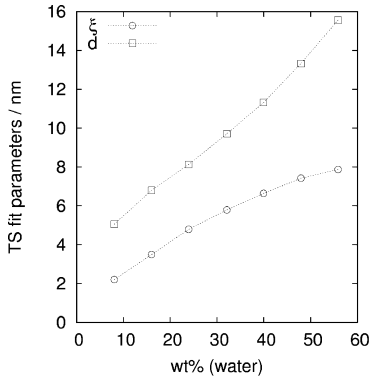

Figure 8. Fit parameters ξ and d of the Teubner–Strey model as a function of the water percent. Dotted lines are only guides to the eyes.

$$\frac{\kappa}{kT} = \frac{10\sqrt{3}\,\pi}{64}\frac{\xi}{d} \tag{14}$$

From this renormalized bending rigidity κ one can calculate the bare bending modulus κ_0 via eq 15, where l_c is the effective thickness of the amphiphilic film, which can be approximated by the length of a single surfactant (which in our case was assumed to be 1.4 nm as estimated from the headgroup area a_h of 0.87 nm^2 (see below) and the molecular surfactant volume of 1.177 nm^3).

$$\frac{\kappa_0}{kT} = \frac{\kappa}{kT} + \frac{3}{4\pi}\ln\left(\frac{d}{2l_c}\right) \tag{15}$$

The obtained data are summarized in Table 1 and show that κ remains roughly constant in the range of 0.4−0.5kT, while κ_0 increases from 0.7kT to 1.0kT. This range of values for the bending constants compares well to values obtained for other nonionic surfactant.[13,48,49] κ goes through a slight maximum in the intermediate regime of water content, which might be due to the different length scales that are probed here. In contrast, the bare bending modulus κ_0 increases with increasing dilution, which can be explained by the fact that originally one starts from amphiphilic monolayers in which the Brij 96 is mixed with butanol, but with increasing dilution the water-soluble butanol is more and more leached out and the remaining amphiphilic monolayer becomes increasingly pure in Brij 96, which, due to its much larger effective length, exhibits a higher rigidity. Thereby this system has an increasingly rigid amphiphilic monolayer and becomes stabilized upon dilution with water.

By applying Porod's asymptotic law

$$\lim_{q\to\infty} I(q) = \frac{2\pi(\Delta\rho)^2}{q^4}\left(\frac{S}{V}\right) \tag{16}$$

we could also determine the specific surface (S/V) of the sample, which then was reverted to the headgroup area requirement per surfactant molecule, by assuming that the surface in the sample separating oily and aqueous parts of the mesostructure is exclusively given by the surfactant. For this calculation we took the scattering length density difference $\Delta\rho$ as obtained from fitting the Teubner–Strey model, where we

Table 1. Values for Correlation Length (ξ), Repeat Distance (d), and Renormalized and Bare Bending Rigidity (κ and κ_0, respectively), as Obtained from Fitting the Teubner-Strey Model to the Experimental SANS Data, and specific area (S/V) and a_h from the Porod Analysis

wt % water	8	16	24	32	40	48	56
ξ/nm	2.20	3.49	4.79	5.79	6.64	7.42	7.87
d/nm	5.05	6.80	8.13	9.71	11.32	13.33	15.56
κ/kT	0.37	0.44	0.50	0.51	0.50	0.47	0.43
κ_0/kT	0.68	0.82	0.92	0.97	1.00	1.01	1.00
(S/V)/nm^{-1}	0.253	0.196	0.193	0.182	0.169	0.148	0.126
a_h/nm^2	1.01 ± 0.07	0.83 ± 0.02	0.87 ± 0.02	0.89 ± 0.02	0.90 ± 0.02	0.88 ± 0.02	0.85 ± 0.02

dx.doi.org/10.1021/la300540d | Langmuir 2012, 28, 10640−10652

always assumed the hydophobic part to be composed of ethyl oleate; the oleyl part of the Brij 96; and the hydrophilic part of D_2O, butanol, and the EO part of the surfactant; and the oil to be constituted of the ethyl oleate, which then yields a value for $\Delta\rho$ of 62.9 × 10^9 cm^{-2}. This Porod analysis leads for all microemulsions to a mean surfactant headgroup area of 87 ± 3 $Å^2$ (for individual values as a function of the water content, see Table 1), indicating that the surface area in the microemulsion is basically given by the steric requirements of the headgroup of the Brij 96, which has been found before by means of DLS measurements to have a headgroup area of 87 $Å^2$,[51] which is in perfect agreement with our findings. A larger deviation is only seen for the microemulsion with 8 wt % water, and this might be explained by the fact that the surfactant is rather well soluble in the oil phase and for this low water content a substantial part of it might be contained in the oily phase, especially as there is not yet enough water present to hydrate the EO head groups efficiently (ratio of $[H_2O]/[EO] = 0.83$).

Though the data are generally well described by the Teubner−Strey model, there are some systematic deviations that are probably due to the simplistic approach of the model and the lack of structural details, for instance that this model assumes that the system is made up of two phases of given scattering length density, separated by a sharp interface. This is not exactly the case here, considering that the surfactant contains a bulky headgroup of 10 EO units. A first hint toward a more complex model can be obtained from the scattering length density differences deduced from the TS-model, which monotonically increase from 3 × 10^{-4} to ca. 6 × 10^{-4} nm^{-2} with increasing water content, while the SLD difference between pure D_2O and ethyl oleate is 6.3 × 10^{-4} nm^{-2}. As expected, the two-phase separation implied in the Teubner−Strey model becomes more realistic for higher water content. In addition, assuming a cubic packing, from the structure peak maximum an average aggregate number density [$^1N = (q_{max}/2\pi)^3$] can be calculated. In that context it should be taken into consideration that from the amounts of water and surfactant contained, an average number of water molecules per EO unit can be calculated, which varies from 0.8 water molecules per EO unit for the microemulsion containing 8% water to 12 D_2O molecules per EO unit for the 56% water microemulsion, suggesting that a large fraction of water is "captured" by the ethylene oxide, even for the highest water content. Finally, it should be noted that the scattering curves for high water content (above 40 wt % water) can be described increasingly well with a model of spherical microemulsion droplets that interact via a repulsive electrostatic interaction potential.

Dynamic Light Scattering. DLS is useful to characterize size and size distribution of microemulsion droplets, as it monitors the collective diffusive motion in colloidally structured systems, provided simple diffusion is the sole mechanism responsible for the variation of the scattered intensity. However, in general, also more complex relaxation mechanisms can be observed that are due to the collective dynamics of a given colloidal system,[52,53] since it can reveal the nature of the relaxation mechanism observed in the intensity autocorrelation function.

Accordingly, the same dilution line studied by SANS (Brij 96/ethyl oleate/butanol microemulsions, with constant ratio between Brij 96/ethyl oleate and butanol of 1.5:1.5:1) and increasing water content, was investigated by measurements performed between 45° and 150°, thereby covering a wide range of scattering vector q. Normalized autocorrelation functions $g^{(2)}(\tau)$ recorded at different scattering vectors for the Brij 96/butanol/ethyl oleate microemulsion, with a water content of 16 wt % water are shown in Figure 9, and the other

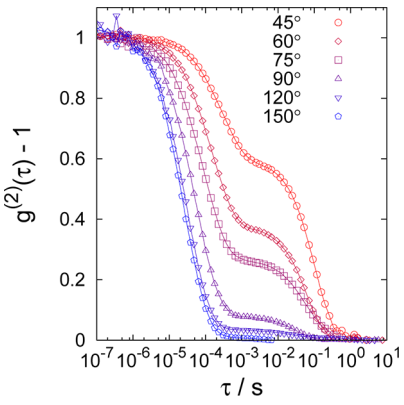

Figure 9. Normalized intensity autocorrelation function $g^{(2)}(\tau)$ recorded at different scattering vectors, for a Brij 96/ethyl oleate/butanol (1.5:1.5:1 by weight) microemulsion and a water content of 16 wt % water. Lines are only guides to the eye.

studied weight percent systems, viz., 24−56, are shown in Figures S6−S10 (Supporting Information). In addition, normalized autocorrelation functions $g^{(2)}(\tau)$ recorded at 60° for microemulsion with different water content are given in Figure 10.

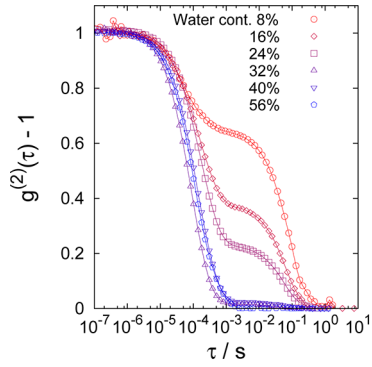

Figure 10. Normalized intensity autocorrelation functions $g^{(2)}(\tau)$ recorded at 60°, for Brij 96/ethyl oleate/butanol (1.5:1.5:1 by weight) microemulsions and increasing water content. Lines are only guides to the eye.

Common microemulsions usually show a monoexponential, diffusive decay.[1] This is not the case here and for all samples containing less than 40 wt % water we always observe a bimodal decay (see Supporting Information, Figures S6−10), where the slower relaxation typically is about 2−3 orders of magnitude slower than the fast one. As a general trend, the amplitude of the slow decay increases with decreasing water content and scattering vector q (at lower q one focuses more on larger structural phenomena, and accordingly one sees their slower relaxation more prominently), until it eventually disappears for the microemulsions containing more than 40 wt % water. These trends are visualized in Figure 11, where the relative importance B (analyzed with eq 5) of the slow decay is reported as a function of the magnitude of the scattering vector (q) for constant water content and as a function of the water content for constant q.

dx.doi.org/10.1021/la300540d | Langmuir 2012, 28, 10640−10652

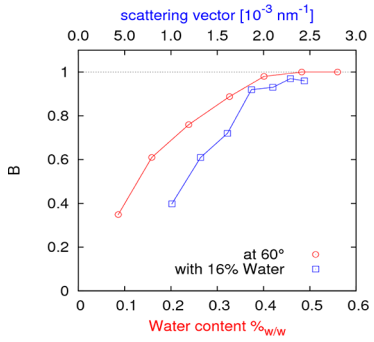

Figure 11. Amplitude of the slow decay (B) as a function of the magnitude of the scattering vector q at constant water content of 16 wt % water and as a function of the water content at constant q = 0.0132 nm^{-1} (corresponding to a characteristic distance of 475 nm). Lines are only guides to the eye.

In that context it should be noted that bimodal relaxation processes in microemulsions have been reported before, for instance by Roux et al.[54] for the microemulsion system SDS/octanol/octane/brine, where the slow relaxation mode was attributed to a thermally activated topological relaxation that is also predicted by theory and controlled by the activation energy of making connections between droplets, which in turn is determined by the bending moduli of the surfactant layer.[55]

Additional information on the nature of the relaxation processes can be obtained from the power-law dependence ($\Gamma \sim q^{-\delta}$) of the relaxation rate Γ on the scattering vector q as a function of the water content (see Figure S10, Supporting Information). Here, one can clearly see that the fast decay is due to simple Brownian diffusion (δ = 2) only at high water content (>40 wt % water), whereas at lower water content δ approaches a value of 3, as usually found for entangled polymer solutions or membrane/bilayer fluctuations.[56,57] Concerning the slow-decay one observes a pronounced increase of δ with increasing water content.

A more comprehensive picture of the system is obtained by looking at the dependence of the fast and slow decay times obtained at a constant angle as a function of the water content of the microemulsion (Figure 12). Here one sees that both relaxation rates remain rather constant and apparently mostly their amplitude (as well as the power law exponent δ) varies as a function of water content.

Via eqs 5 and 6, assuming that the medium is the oil phase with a viscosity of 5.15 cP (ethyl oleate) and the water phase has a viscosity of 0.89 cP for the microemulsions with 8 and 56% water content, respectively, one obtains hydrodynamic radii in the range of 2−10 nm from the fast decay, in good agreement with the SANS findings. Apparently at these limiting situations the system is rather well described by such a simple droplet picture. Concerning the slow decay, it would correspond to diffusing particles with a hydrodynamic radius of ca. 1 μm. This is in apparent contradiction to the results of the average intensity of the dynamic light scattering and SANS, as such big aggregates would cause a rapid increase in scattering intensity at low q, and this was not detected by our experiments. Therefore, we can conclude that at low and intermediate water content (15−40 wt % water) effectively a network is formed (presumably of percolated microemulsion aggregates) and free diffusion of the individual aggregates is suppressed. The slow relaxation observed in this range is apparently linked to the existence of such a percolated microemulsion network. With increasing water content this network then is destroyed due to the formation of disconnected O/W droplets, where the particles then can diffuse freely.

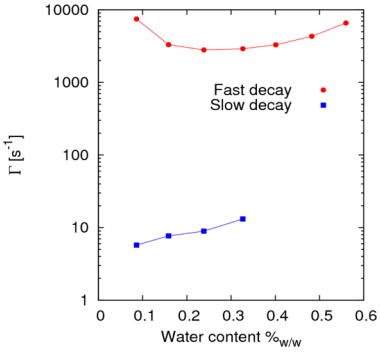

Figure 12. Dependence of the fast (○) and slow (□) relaxation rates (from fitting eq 5) obtained at 60° on the water content of the microemulsion. Lines are only guides to the eye.

Nuclear Magnetic Resonance. NMR has been established as a powerful and reliable method for the investigation of surfactant aggregates.[58−60] Different 1D and 2D NMR techniques have been successfully applied to study both static (micelle size and shape, degree of association, structure) and dynamic properties (molecular mobility, kinetics of micelle formation) of surfactant systems. The 2D-ROESY experiment is a widely accepted technology to measure the dipolar interactions between protons. The microstructural changes in the microemulsions can be outlined to a certain extent, although it is difficult to determine the precise interproton distances between each individual proton from the cross-peak intensities of the ROESY spectrum.[61,62] 2D-ROESY spectroscopic analysis has been used to study the microstructure of the Brij 96/ethyl oleate/butanol microemulsions. Also the ^{1}H NMR spectra has been utilized to get information about the interaction between the molecules. These studies help in providing an insight into the dissolution behavior of the added water molecules in the microemulsion and the effect of water on the microenvironment of the microemulsions.[63] The microemulsions of different weight percent (using D_2O) have been selected from different regions, i.e., W/O, bicontinuous, O/W, on the basis of results of viscosity. ^{1}H NMR spectrum of microemulsion is the cumulative spectrum of all the components. ^{1}H NMR spectra of pure components and microemulsions are depicted in Figures S1 and 12−14 (Supporting Information). Some of the peaks overlap in the microemulsions except that of vinylic protons of ethyl oleate (Figure S14a−e, Supporting Information). It has been found that the chemical shifts of microemulsions for all the six studied weight percent show a downfield shift in comparison to the pure components. Downfield shifts in microemulsions with respect to its components give an evidence of interhydrogen bonding. A hydrogen binding network is created between butanol, ethyl oleate, and the oxyethlene groups of Brij 96, which makes the interface layer more firm.[64] It has also been observed that as the percentage of D_2O increases, the chemical shifts of the microemulsions show upfield. This is probably due to lesser hydrogen bonding experienced in the presence of D_2O.

Further, to ascertain the role of added water on the microstructure of the microemulsion, 2D-ROESY has been utilized (Figure 13a−f). The cross peak of the microemulsion

dx.doi.org/10.1021/la300540d | Langmuir 2012, 28, 10640−10652

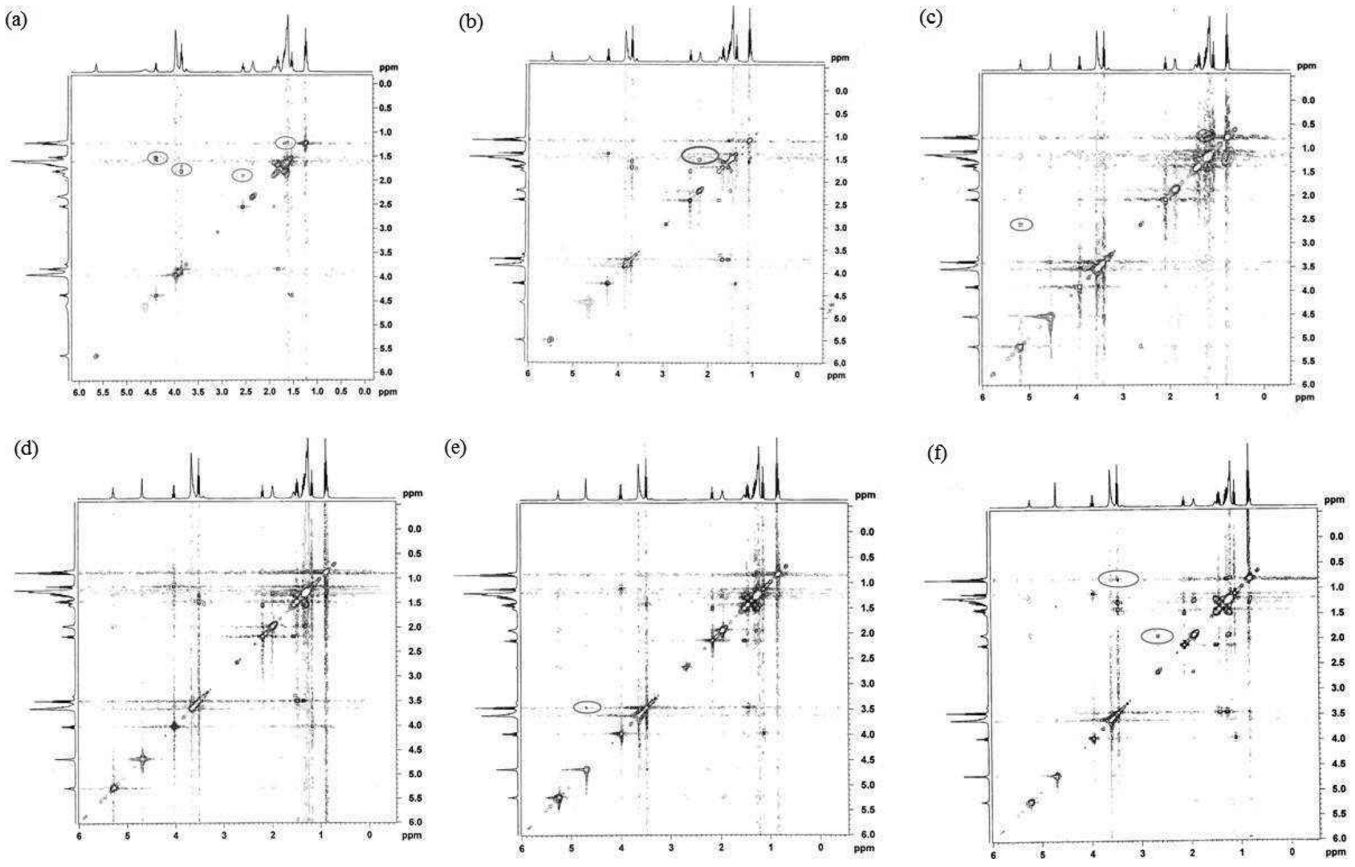

Figure 13. ROESY spectra of Brij 96 microemulsion in D_2O at various weight percent: (a) 8.5, (b) 14.6, (c) 27.0, (d) 31.9, (e) 39.6, and (f) 48.3. (Larger versions of these spectra are given in the Supporting Information, Figure S15a–f.)

with 8.5 wt % water shows many interproton correlations among surfactant, oil, and butanol. Figure 13a shows the interaction of $O-CH_2$ of ethyl oleate with CH_2 of surfactant tails. The correlation peak also exists between butanol and CH_2 of ethyl oleate and surfactant tails. It is the ester end that is interacting with the aliphatic part of Brij 96 ($C_{18}H_{35}$) and the oxyethylene group of Brij 96 (OCH_2CH_2) with CH_2 of oil, as evident from the correlation peak. The correlation peaks are also observed within ethyl oleate for CH_2 with CH_3 and OCH_2. On the basis of NMR results, a probable structure has been proposed (Scheme 1) which shows that ethyl oleate gets entangled around the hydrophobic tails of surfactant with butanol molecules mainly at the interface. This is a bit of a surprising conformation but might be explainable by the fact that the ethyl oleate with its cis double bond has a natural tendency for bending and therefore might be prone to filling the region directly below the headgroup, where naturally some lack of material will be present (as in every surfactant the headgroup area is much larger than volume/area requirement of the following alkyl chain.).

Scheme 1. Probable Microstructure of Microemulsion Given by NMR Studies

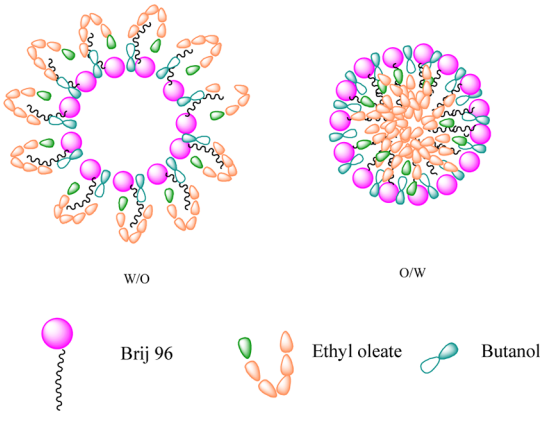

As the content of D_2O increases, along with the earlier correlation peaks a new peak emerges between the CH_2-O-CH_2 of Brij 96 and the CH_2 chain of ethyl oleate. In case of the bicontinuous region in the Brij microemulsion (27 and 31.9 wt % water), the emergence of a new peak (butanol with D_2O) and disappearance of another (end of oil $O-CH_2$ with surfactant) show the movement of surfactant and cosurfactant molecules (owing to the rearrangement in bicontinuous phase from W/O). The sample with 39 wt % water shows an arrangement similar to that in the droplet form. Ethylene group interactions are more prominent in these regions, as indicated from the presence of correlation peaks similar to the ones present in W/O type region.

In case of O/W microemulsion at 48.3 wt % of water, the interactions between butanol with D_2O and CH_2 of Brij 96 decrease. Only a correlation peak of butanol with oil exists, which is due to the presence of more cosurfactant in the oil droplet. More correlation is observed between $-CH_2COO-$ and CH– adjacent to the double bond (Figures 13e,f). This provides evidence of interaction of the ester group of ethyl oleate with the vinylic hydrogens of Brij.

dx.doi.org/10.1021/la300540d | *Langmuir* 2012, 28, 10640–10652

CONCLUSIONS

In the present work, we investigated microemulsions with the pharmaceutically/cosmetically relevant oil ethyl oleate, which were formulated with Brij 96 (oleyl$(EO)_{10}$) as surfactant and mainly butanol as cosurfactant. These investigations were carried out along a dilution line with water in order to elucidate the structural transitions upon water dilution, as it might also be frequently relevant in applications of such formulations. The characterization was carried out using viscosity, surface tension, 2D-ROESY NMR, SANS, DLS, and cyclic voltammetry. From these experiments it can be concluded that the Brij 96/butanol/ethyl oleate system forms a U-type microemulsion system that undergoes a continuous transition from swollen micelles to W/O droplets (6 wt %) which percolate and thereby form a bicontinuous structure (∼20 wt %) that upon further addition of water is reverted into a finally present O/W droplet structure (>48 wt % water).

SANS experiments show a continuous increase of the structural units upon dilution with water. At the same time the bare bending modulus κ increases somewhat, presumably due to less butanol contained in the interface, and this increased monolayer rigidity supports the stability of the formed microemulsion structure. In addition, the microstructure of the studied microemulsion has been characterized by cyclic voltammetry using ferrocene as electroactive probe, which shows a pronounced maximum of the diffusivity in the bicontinuous range. Furthermore, these experiments gave a deeper insight into the unusual behavior of ferrocene electrochemistry in the microheterogeneous environment. In contrast, DLS studies showed a rather complex behavior, where only for the water-rich O/W side a simple diffusive behavior is observed that corresponds to the droplet size obtained by SANS. For lower water content, a second relaxation mechanism is seen that becomes more prominent with decreasing water concentration, while the fast relaxation is only little affected by the extent of dilution. This slow relaxation is attributed to the presence of a network of percolated microemulsion aggregates. This network formation may be attributed to the amphiphilicity of the oil employed that may make such network formation easier. The 2D-ROESY studies complete this picture by giving an insight about the molecular arrangement and concluded that ethyl oleate mainly gets entangled around the hydrophobic tails of surfactant with butanol molecules mainly lying at the interface. An interesting observation is that apparently the methyl end of the ethyl oleate is on average close to the amphiphilic interface. This can be explained by the fact that the oleate is of bent shape and in addition the alkyl end might have a propensity to sit close the amphiphilic interface in order to fill the packing hole present there. It should also be noted that upon further water addition the system will phase separate and apparently here an emulsion is formed. In that respect, it exhibits some similarities to PIC (phase inversion concentration) nanoemulsions, where one also may observe first the formation of a microemulsion, which is followed upon further water addition by a thermodynamically instable nanoemulsion.[65−67] A similar situation might be present here but with a shorter time range of metastability for the higher water content. This is not a very common finding, as most surfactant oil mixtures tend to a rather quick disintegration upon water addition, but due to the high butanol content and the rather polar oil ethyl oleate one has in principle similar conditions as for typical PIC nanoemulsions. The potential for nanoemulsion formation might be interesting for additional applications of such Brij 96/butanol/ethyl oleate systems.

In summary, our findings shed substantial further light on the structure and properties of microemulsions formed with oils that are relevant for pharmaceutical and cosmetical formulations. As the oil employed (ethyl oleate) has some more complex properties than a simple hydrocarbon, also the phase behavior and the structures formed are somewhat more complex, for instance, by forming interconnected networks over an extended range in the phase diagram, but in general, they follow trends expected for such systems. Yet, this network formation induced by percolation will have relevance for the delivery properties of corresponding formulations, and in general, our findings should be of relevance for a more systematic formulation of such rather complex microemulsion systems.

ASSOCIATED CONTENT

Supporting Information

^{13}C NMR of Brij 96 in D_2O, MS of Brij 96, optical inspection of Brij 96/ethyl oleate/butanol microemulsions, plot of $1/\eta(d\eta/d(\text{wt \% water})$ and $d\gamma/d(\text{wt \% water})$ vs wt % water for the Brij 96/ethyl oleate/butanol system, cyclic voltammograms of ferrocene in Brij 96/butanol/ethyl oleate, normalized intensity autocorrelation functions $g^{(2)}(\tau)$ recorded at different scattering vectors for different weight fractions of water, dependence of the exponent δ of the relaxation rate Γ of the DLS curves on the magnitude of the scattering vector q ($\Gamma \sim q^{-\delta}$) as a function of the water content, ^1H NMR spectrum of pure components and microemulsions for different weight fractions of water, and enlarged view of the ROESY spectra given in the text. This material is available free of charge via the Internet at http://pubs.acs.org/.

AUTHOR INFORMATION

Corresponding Author

*E-mail: michael.gradzielski@tu-berlin.de, skmehta@pu.ac.in.

Notes

The authors declare no competing financial interest.

ACKNOWLEDGMENTS

This research work was partially supported by the DAAD-DST project (DST/INT/DAAD/P-177/2008) and CSIR New Delhi. Allocation of SANS beamtime from the Institute Laue-Langevin (ILL) is gratefully acknowledged. We would also like to thank the three referees for a number of constructive suggestions that certainly improved the quality of our paper.

REFERENCES

(1) Kumar, P., Mittal, K. L. *Handbook of Microemulsion: Science and Technology*; Marcel Dekker, New York, 1999.

(2) Hoar, T. P.; Schulman, J. H. Transparent water-in-oil dispersions: The oleopathic hydro-micelle. *Nature* **1943**, *152*, 102−103.

(3) Gupta, S. Biocompatible microemulsion systems for drug encapsulation and delivery. *Curr. Sci.* **2011**, *101*, 174−188.

(4) Scriven, L. E. In *Micellization, Solubilization and Microemulsion*; Mittal, K. L., Ed.; Plenum Press: New York, 1977; Vol. 2, pp 877.

(5) Leung, R.; Shah, D. O. Solubilization and Phase equilibria of water-in-oil microemulsions. *J. Colloid Interface Sci.* **1987**, *120*, 330−345.

(6) Kahlweit, M.; Strey, R. Phase behavior of ternary system of the type water-oil-nonionic amphiphilies (microemulsions). *Angew. Chem.* **1985**, *97*, 655−669.

(7) Strey, R. Microemulsion microstructure and interfacial curvature. *Colloid Polym. Sci.* **1994**, *272*, 1005−1019.
(8) Helfrich, W. Z. Elastic properties of lipid bilayers—Theory and possible experiments. *Naturforsch* **1978**, *28*, 693−703.
(9) De Gennes, P. G.; Taupin, C. Microemulsions and the flexibility of oil/water interface. *J. Phys. Chem.* **1982**, *86*, 2294−2304.
(10) Cates, M. E.; Andelman, D.; Safran, S. A.; Roux, D. Theory of microemulsions: Comparison with experimental behavior. *Langmuir* **1988**, *4*, 802−806.
(11) Langevin, D. Micelles and microemulsions. *Annu. Rev. Phys. Chem.* **1992**, *43*, 341−369.
(12) Jouffroy, J.; Levinson, P.; De Gennes, P. G. Phase equilibria involving microemulsions (Remarks on the Talmon−Prager model). *J. Phys. (Paris)* **1982**, *43*, 1241−1248.
(13) Gradzielski, M.; Langevin, D.; Farago, B. Experimental investigation of the structure of nonionic microemulsions and their relation to the bending elasticity of the amphiphilic film. *Phys. Rev. E* **1996**, *53*, 3900−3919.
(14) Lawrence, M. J.; Rees, G. D. Microemulsion-based media as novel drug delivery systems. *Adv. Drug Delivery Rev.* **2000**, *5*, 89−121.
(15) Clausse, M.; L. Nicolas-Morgantini, Zradba, A.; D.TouraudIn *Microemulsion Systems*; Rosano, H. L.; Clausse, M., Eds.; Marcel Dekker: New York, 1988; p 15.
(16) Bagwe, R. P.; Kanicky, J. R.; Palla, B. J.; Patanjali, P. K.; Shah, D. O. Improved drug delivery using microemulsions: Rationale, recent progress, and new horizons. *Crit. Rev. Ther. Drug Carrier Syst.* **2001**, *18*, 77−140.
(17) Kahlweit, M.; Strey, R.; Haase, D.; Kunieda, H.; Schmeling, T.; Faulhauber, B.; Borkovec, M.; Eicke, H. F.; Busse, G.; Eggers, F.; Funck, T.; Richmann, H.; Magid, L.; Söderman, O.; Stilbs, P.; Winkler, J.; Dittrich, A.; Jahn, W. How to study microemulsions. *J. Colloid Interface Sci.* **1987**, *118*, 436−453.
(18) Podlogar, F.; Rogac, M. B.; Gasperlin, M. The effect of internal structure of selected water−Tween 40−Imwitor 308−IPM microemulsions on ketoprofene release. *Int. J. Pharm.* **2005**, *302*, 68−77.
(19) Gradzielski, M. Recent developments in the characterisation of microemulsions. *Curr. Opin. Colloid Interface Sci.* **2008**, *13*, 263−269.
(20) Kogan, A; Garti, N. Microemulsions as transdermal drug delivery vehicles. *Adv. Colloid Interface Sci.* **2006**, *123−126*, 369−385.
(21) Gradzielski, M. Effect of the cosurfactant structure on the bending elasticity in nonionic oil-in-water microemulsions. *Langmuir* **1998**, *14*, 6037−6044.
(22) Nandi, I.; Bari, M.; Joshi, H. Study of isopropyl myristate micro emulsion system containing cyclodextrin to improve solubility of 2 model, hydrophobic drugs. *AAPS PharmSciTech.* **2003**, *4*, 1−9.
(23) Shevachman, M.; Garti, N.; Shani, A.; Sintov, A. C. Enhanced percutaneous permeability of diclofenac using a new U-type dilutable microemulsion. *Drug Dev. Ind. Pharm.* **2008**, *34*, 403−412.
(24) Junyaprasertа, V. B.; Boonme, P.; Songkro, S.; Krauel, K.; Rades, T. Transdermal delivery of hydrophobic and hydrophilic local anesthetics from o/w and w/o Brij 97-based microemulsions. *J. Pharm. Pharmaceut. Sci.* **2007**, *10*, 288−298.
(25) Junyaprasert, V. B.; Boonsaner, P.; Leatwimonlak, S.; Boonme, P. Enhancement of the skin permeation of clindamycin phosphate by Aerosol OT/1-butanol microemulsions. *Drug Dev. Ind. Pharm.* **2007**, *33*, 874−880.
(26) Moerlein, S. M.; Gaehle, G. G.; Lechner, K. R.; Bera, R. K.; Welch, M. J. Automated production of oxygen-15 labeled butanol for PET measurement of regional cerebral blood flow. *Appl. Radiat. Isotopes* **1993**, *44*, 1213−1218.
(27) Engelskirchen, S.; Elsner, B.; Sottmann, T.; Strey, R. Triacylglycerol microemulsions stabilized by alkyl ethoxylate surfactants—A basic study: Phase behavior, interfacial tension and microstructure. *J. Colloid Interface Sci.* **2007**, *312*, 114−121.
(28) Barth, A.; Heunemann, P.; Prevost, S.; Gradzielski, M. Solubilisation of different medium chain esters in zwitterionic surfactant solutions—Effects on phase behaviour and structure. *J. Colloid Interface Sci.* **2011**, *364*, 148−156.
(29) Mehta, S. K.; Kaur, G.; Mutneja, R.; Bhasin, K. K. Solubilization, microstructure, and thermodynamics of fully dilutable U-type Brij microemulsion. *J. Colloid Interface Sci.* **2009**, *338*, 542−549.
(30) Jacrot, B. The study of biological structures by neutron scattering from solution. *Rep. Prog. Phys.* **1976**, *39*, 911−953.
(31) Keiderling, U. The new 'BerSANS-PC' software for reduction and treatment of small angle neutron scattering data. *Appl. Phys. A: Mater. Sci. Process.* **2002**, *74*, 1455−1457.
(32) Kissinger, P. T.; Heineman, W. R. Cyclic voltammetry. *J. Chem. Educ.* **1983**, *60*, 702−706.
(33) Platz, G.; Thunig, C.; Hoffmann, H. Phase behavior of alkyl polyglycosides in combination with fatty alcohols and alkyl sulphates. *Ber. Bunsenges. Phys. Chem.* **1992**, *96*, 667−677.
(34) Hoffmann, H.; Thunig, C.; Munkert, U.; Meyer, H. W.; Richter, W. From vesicles to the L3 (sponge) phase in alkyldimethylamine oxide/heptanol systems. *Langmuir* **1992**, *8*, 2629−2638.
(35) Fanun, M. Conductivity, viscosity, NMR and diclofenac solubilization capacity studies of mixed nonionic surfactants microemulsions. *J. Mol. Liq.* **2007**, *135*, 5−13.
(36) Scriven, L. E. Equilibrium bicontinuous structure. *Nature* **1976**, *263*, 123−125.
(37) Talmon, Y.; Prager, S. Statistical mechanics of microemulsions. *Nature* **1977**, *267*, 333−35.
(38) Martino, A.; Kaler, E. W. Phase behavior and microstructure of nonaqueous microemulsions. *Langmuir* **1995**, *11*, 779−784.
(39) Gradzielski, M.; Hoffmann, H. Rheological properties of microemulsions. In *Handbook of Microemulsion Science and Technology*; Kumar, P., Mittal, K. L., Eds.; Marcel Dekker Inc., New York, 1999; Chapter 1.
(40) Quemada, D.; Langevin, D. Rheological modelling of microemulsions. *J. Theor. Appl. Mech. Num. Spec.* **1985**, 201−237.
(41) Garti, N.; Yaghmur, A.; Leser, M. E.; Clement, V.; Watzke, H. J. Improved oil solubilization in o/w food-grade microemulsions in the presence of polyols and ethanol. *J. Agric. Food Chem.* **2001**, *49*, 2552−2562.
(42) Leitao, S.; Somoza, A. M.; Telo da Gama, M. M.; Sottmann, T.; Strey, R. Scaling of the interfacial tension of microemulsions: A phenomenological description. *J. Chem. Phys.* **1996**, *105*, 2875−2883.
(43) Mo, C.; Zhong, M.; Zhong, Q. Investigation of structure and structural transition in microemulsion systems of sodium dodecyl sulfonate + *n*-heptane + *n*-butanol + water by cyclic voltammetric and electrical conductivity measurements. *J. Electroanal. Chem.* **2000**, *493*, 100−107.
(44) Guering, P.; Lindman, B. Droplet and bicontinuous structures in microemulsions from multicomponent self-diffusion measurements. *Langmuir* **1985**, *1*, 464−468.
(45) Jha, B. K.; Kulkarni, B. D.; Vinod, M. P.; Vijayamohanan, K. An unusual electron-transfer behavior of ferrocene in aqueous microemulsion systems. *Chem. Phys. Lett.* **1995**, *240*, 442−448.
(46) Teubner, M.; Strey, R. Origin of the scattering peak in microemulsions. *J. Chem. Phys.* **1987**, *87*, 3195−3200.
(47) Chen, S. H.; Chang, S. L.; Strey, R.; Samseth, J.; Mortensen, K. Structural evolution of bicontinuous microemulsions. *J. Phys. Chem.* **1991**, *95*, 7427−7432.
(48) Sottmann, T.; Strey, R.; Chen, S.-H. A small-angle neutron scattering study of nonionic surfactant molecules at the water−oil interface: Area per molecule, microemulsion domain size, and rigidity. *J. Chem. Phys.* **1997**, *106*, 6483−6491.
(49) Gradzielski, M.; Langevin, D.; Sottmann, T.; Strey, R. Small angle neutron scattering near the wetting transition: Discrimination of microemulsions from weakly structured mixtures. *J. Chem. Phys.* **1996**, *104*, 3782−3787.
(50) Pieruschka, P.; Safran, S. A.; Marcelja, S. T. Fluctuating interfaces in microemulsion and sponge phases. *Phys. Rev. E* **1995**, *52*, 1245−1247.
(51) Yaghmur, A.; Aserin, A.; Antalek, B.; Garti, N. Microstructure considerations of new five-component Winsor IV food-grade microemulsions studied by pulsed gradient spin−echo NMR, conductivity, and viscosity. *Langmuir* **2003**, *19*, 1063−1068.

(52) Ngai, K. L.; Phillies, G. D. J. Coupling model analysis of polymer dynamics in solution: Probe diffusion and viscosity. *J. Chem. Phys.* **1996**, *105*, 8385−8397.
(53) Tsianou, M.; Kjøniksen, A.-L.; Thuresson, K.; Nyström, B. Light scattering and viscoelasticity in aqueous mixtures of oppositely charged and hydrophobically modified polyelectrolytes. *Macromolecules* **1999**, *32*, 2974−2982.
(54) Peter, U.; Roux, D.; Sood, A. K. Observation of a topological relaxation mode in microemulsions. *Phys. Rev. Lett.* **2001**, *86*, 3340−3343.
(55) Milner, S. T.; Cates, M. E.; Roux, D. Hydrodynamic modes and topology in microemulsions and L3 phases. *J. Phys. (Paris)* **1990**, *51*, 2629−2639.
(56) Hoffmann, I.; Heunemann, P.; Prévost, S.; Schweins, R.; Wagner, N. J.; Gradzielski, M. Self-aggregation of mixtures of oppositely charged polyelectrolytes and surfactants studied by rheology, dynamic light scattering and small-angle neutron scattering. *Langmuir* **2011**, *27*, 4386−4396.
(57) Nystroem, B.; Lindman, B. Dynamic and viscoelastic properties during the thermal gelation process of a nonionic cellulose ether dissolved in water in the presence of ionic surfactants. *Macromolecules* **1995**, *28*, 967−974.
(58) Shimizu, S.; Pires, P. A. R.; Seoud, O. A. E. ^{1}H and ^{13}C NMR Study on the aggregation of (2-acylaminoethyl)trimethylammonium chloride surfactants in D_2O. *Langmuir* **2003**, *19*, 9645−9652.
(59) Alonso, B.; Harris, R. K.; Kenwright, A. M. Micellar solubilization: Structural and conformational changes investigated by ^{1}H and ^{13}C liquid-state NMR. *J. Colloid Interface Sci.* **2002**, *251*, 366−375.
(60) Gjerde, M.; Nerdal, W.; Holand, H. A NOESY NMR study of the interaction between sodium dodecyl sulfate and poly(ethylene oxide). *J. Colloid Interface Sci.* **1996**, *183*, 285−288.
(61) Yuan, H. Z.; Zhao, S.; Cheng, G. Z.; Zhang, L.; Miao, X. J.; Mao, S. Z.; Yu, J. Y.; Shen, L. F.; Du, Y. R. Mixed micelles of Triton X-100 and cetyl trimethylammonium bromide in aqueous solution studied by ^{1}H NMR. *J. Phys. Chem. B* **2001**, *105*, 4611−4615.
(62) Yuan, H. Z.; Cheng, G. Z.; Zhao, S.; Miao, X. J.; Yu, J. Y.; Shen, L. F.; Du, Y. R. Conformational dependence of Triton X-100 on environment studied by 2D NOESY and ^{1}H NMR relaxation. *Langmuir* **2000**, *16*, 3030−3035.
(63) Gao, Y. A.; Li, N.; Zheng, L. Q.; Bai, X. T.; Yu, L.; Zhao, X. Y.; Zhang, J.; Zhao, M. W.; Li, Z. Role of solubilized water in the reverse ionic liquid microemulsion of 1-butyl-3-methylimidazolium tetrafluoroborate/tx-100/benzene. *J. Phys. Chem. B* **2007**, *111*, 2506−2513.
(64) Gao, Y.; Hilfert, L.; Voigt, A.; Sundmacher, K. Decrease of droplet size of the reverse microemulsion 1-butyl-3-methylimidazolium tetrafluoroborate/triton x-100/ cyclohexane by addition of water. *J. Phys. Chem. B* **2008**, *112*, 3711−3719.
(65) Solè, I.; Maestro, A.; González, C.; Solans, C.; Gutiérrez, J. M. Optimization of nano-emulsion preparation by low-energy methods in an ionic surfactant system. *Langmuir* **2006**, *22*, 8326−8332.
(66) Sonneville-Aubrun, O.; Babayan, D. Bordeaux, D.; Lindner, P.; Rata, G.; Cabane, B. Phase transition pathways for the production of 100 nm oil-in-water emulsions. *Phys. Chem. Chem. Phys.* **2009**, *11*, 101−110.
(67) Heunemann, P.; Prévost, S.; Grillo, I.; Marino, C. M.; Meyer, J.; Gradzielski, M. A comparative study on switchable adhesion between thermoresponsive polymer brushes on flat and rough surfaces. *Soft Matter* **2011**, *7*, 5697−5710.